Zurriaga Carda, J.; Lastra, ML.; Antolinos-Turpin, CM.; Morales-Román, RM.; Sancho-Tello, M.; Perea-Ruiz, S.; Milián, L.... (2020). A cell-free approach with a supporting biomaterial in the form of dispersed microspheres induces hyaline cartilage formation in a rabbit knee model. Journal of Biomedical Materials Research Part B Applied Biomaterials. 108(4):1428-1438. https://doi.org/10.1002/jbm.b.34490

A cell-free approach with a supporting biomaterial in the form of dispersed microspheres induces hyaline cartilage formation in a rabbit knee model

Javier Zurriaga Carda[1,2], Maria Laura Lastra[3], Carmen María Antolinos-Turpin[4], Rosa María Morales-Román[4], María Sancho-Tello[1,5], Sofía Perea-Ruiz[4], Lara Milián[1,5], Juan Manuel Fernandez[3], Ana Maria Cortizo[3], Carmen Carda[1,5,6], Gloria Gallego Ferrer[4,6], José Luis Gómez Ribelles[4,6*]

1. *Departamento de Patología, Facultad de Medicina y Odontología, Universitat de València, Valencia, Spain.*
2. *Hospital IMED, Valencia, Spain.*
3. *Laboratorio de Investigaciones en Osteopatías y Metabolismo Mineral (LIOMM), Facultad de Ciencias Exactas, Universidad Nacional de La Plata 47 y 115 (1900), Argentina.*
4. *Center for Biomaterials and Tissue Engineering (CBIT), Universitat Politècnica de València, Valencia, Spain.*
5. *INCLIVA Biomedical Research Institute, Valencia, Spain.*
6. *Biomedical Research Networking Center on Bioengineering, Biomaterials and Nanomedicine (CIBER-BBN), Valencia, Spain.*

(*) Corresponding author:

Name: José Luis Gómez Ribelles

e-mail: jlgomez@ter.upv.es

Center for Biomaterials and Tissue Engineering (CBIT), Universitat Politècnica de València, Valencia, Camino de Vera s/n 46022 Valencia, Spain

Abstract:

The objective of this study was to test a regenerative medicine strategy for the regeneration of articular cartilage. This approach combines microfracture of the subchondral bone with the implant at the site of the cartilage defect of a supporting biomaterial in the form of microspheres aimed at creating an adequate biomechanical environment for the differentiation of the mesenchymal stem cells that migrate from the bone marrow. The possible inflammatory response to these biomaterials was previously studied by means of the culture of RAW264.7 macrophages. The microspheres were implanted in a defect of 3 mm in diameter in the trochlea of the femoral condyle of New Zealand rabbits, covering them with a PLLA membrane manufactured by electrospinning. Experimental groups included a group where exclusively poly(L-lactic acid) (PLLA) microspheres were implanted, another group where a mixture of 50/50 microspheres of PLLA, (hydrophobic and rigid) and others of chitosan, CHT, (a hydrogel) were used, and a third group used as a control where no material was used and only the membrane was covering the defect. The histological characteristics of the regenerated tissue have been evaluated three months after the operation. We found that during the regeneration process the microspheres, and the membrane covering them, are displaced by the neoformed tissue in the regeneration space towards the subchondral bone region, leaving room for the formation of a tissue with the characteristics of hyaline cartilage.

Keywords: Articular cartilage regeneration, cartilage engineering, rabbit knee model, polylactide, chitosan, microspheres

Running title: Microspheres for a cell free approach for cartilage regeneration

Introduction

Cartilage regeneration is a problem yet to be solved in clinical practice, since it is a tissue with a low cell density and without vascularization. Osteochondral injuries often result in articular cartilage damage and premature osteoarthritis. This is already a huge problem, as it has been described to affect over 10,2% of adult population [1], and its effect is noted in a 5-fold increase of articular prosthesis implanted in the period between 1994 and 2005 [2].

In clinical practice, a series of techniques have been applied for the regeneration or repair of articular cartilage that do not require the manipulation of cells outside the patient's organism, such as microfracture [3], mosaicplasty [4]. Other techniques based on tissue engineering require the implant of chondrocytes (autologous chondrocyte implantation, ACI, or matrix-assisted chondrocyte implantation, MACI) [5] or mesenchymal stem cells, MSCs, expanded *ex vivo*.

Cell-free approaches based on injuring subchondral bone to induce migration of pluripotent cells with chondrogenic capacity to the site of the defect are cheaper and technically easier to perform, but their intermediate and long-term results are poor, especially for younger and active patients [6]. It has been hypothesized that the implantation of a supporting biomaterial able to create the adequate biomechanical environment for the cells arriving to the regeneration site could significantly improve the quality of the new-formed cartilage. The implantation of cell-free scaffolds for cartilage regeneration greatly simplifies the treatment with respect to the implant of cell laden scaffolds or hydrogels with lower mean costs and fewer surgeries needed, avoiding complications related to two-step techniques [7]. These scaffolds should be non-immunogenic and biodegradable to avoid deposits, porous to allow migration and adhesion of cells from subchondral bone, and mechanically stable to sustain the regeneration process. Bioresorbable polyesters, such as polylactide, PLA [8,9] or polycaprolactone, PCL [10,11] have been used previously in cartilage engineering animal models. Cell-free strategies using PCL [10,11] or biostable acrylic scaffolds of varying stiffness [12,13] probed in rabbit knee models their capacity to induce the formation of histologically high quality tissue with the characteristics of hyaline cartilage. To increase the wettability of these hydrophobic materials their combination with hydrophilic coatings have been proposed [14].

In this work, we studied in a rabbit model the performance of a scaffolding material in the form of microspheres, combining stiff and hydrophobic microspheres made of a bioresorbable material such as PLLA with hydrophilic and compliant chitosan, CHT, microspheres. CHT has

been proved to be a biodegradable and biocompatible material, and has been proposed for cartilage regeneration. Although many works demonstrated good biocompatibility of CHT-scaffolds [15-18], others have reported increased inflammatory response of CHT materials when macrophages were studied [19,20]. This is why the possible inflammatory response was investigated using a model of RAW264.7 macrophages in culture in the presence of PLLA and/or CHT microspheres before implantation in animals.

Materials and Methods

Microspheres obtaining and characterization

PLLA used was medical grade (Purasorb PL-18 by Corbion). PLLA microspheres were fabricated via an oil/water emulsion method. The oil phase consisted of 2% w/v PLLA solution in chloroform and the aqueous phase 4% w/v poly(vinyl alcohol) solution (Mw 130,000 Da, 99% + hydrolized by Sigma Aldrich). Briefly, 20 mL of PLLA solution was added drop wise via a syringe pump into 200 mL of PVA solution under constant stirring at 750 rpm with a feed rate of 1 mL/min. 150 mL of deionized water was added to assist with solvent evaporation, and the mixture was kept stirring during 24 h. After stirring, the resulting microparticles suspension were washed twice with water, filtered with ethanol through a 50 μm filter, air-dried and vacuum dried prior to microparticles collection.

In order to improve the hydrophilicity, the microparticles were subjected to plasma treatment inside a Piccolo (Plasma Electronic) Microwave plasma chamber. The plasma treatment parameters were: Argon gas, 50 Pa initial gas pressure, with a gas flow rate of 160 sccm, during 600 s.

Electrospun PLLA mat was prepared from a 2% w/v PLLA solution in a 30/70 mixture of NN Dimethyl Formamide and Methylene Chloride (Sigma) with a voltage of 25 kV between the needle and the flat collector, with a traveling distance of 15 cm and needle diameter of 0.5 mm, and feeding rate of 8 mL/h.

CHT, microspheres were formed by neutralization of an acid solution of CHT in a basic solution subjected to an electric field. Medical-grade CHT (Protasan UP B 80/20, Novamatrix) was dissolved at a concentration of 2.5% w/v in a 2 % v/v acetic acid solution. The precipitating solution was prepared with NaOH 1M, $Na_2SO_4 \cdot 10\ H_2O$ 0.5 M and distilled water in a ratio 10/30/60 and mixed with absolute ethanol in a proportion 70/30 to get better dispersion of the beads. The process consisted in passing the solution through a needle of 0.2 mm inner diameter,

placed at a height of 7 cm over the coagulant bath in agitation, with constant feed ratio of 70 μL/min controlled by a syringe pump. A continuous electric field of 6 kV was applied between the needle and the bottom of the coagulating bath, performing the process inside an Encapsulation Unit VARV1 (Nisco Enginering).

CHT microspheres were washed with distilled water several times until pH≈7, by decantation and aspiration of the supernatant.

Confined compression tests were performed in a Microtest Electromecánica SCM3000 95 instrument. Prior to the test, the microspheres were kept immersed in liquid water for 24 h. The microspheres were introduced in a plunger cylinder device, made of PTFE, with a diameter of 5 mm. The initial thickness of the microsphere layer was 1 mm. The cylinder had perforations in the lower part that allow eliminating the water that comes out of the microspheres during the compression test. A deformation ramp was applied at a speed of 1 mm/min until the force measured in the load cell was 10 N. The result expressed in terms of a compression module, *K*, is the average of 5 measurements on a confined cylindrical sample of cross section *S*, and initial height l_0

$$K = \frac{F/S}{\Delta l/l_0}$$

where F is the applied compression force, and Δl is the measured deformation.

The morphology of PLLA microparticles was observed in the Field Emission Scanning Electron Microscopy (FESEM) (Ultra 55, Zeiss Auriga Compact, Germany). The images were taken at 1 kV, with platinum coated samples (JFC 1100, JEOL, Japan device). Images of the CHT microspheres, swollen in water, were obtained by binocular loupe (MZ APO, Leica Microsystems, Germany).

Raw264.7 culture and incubations. Evaluation of Cytotoxicity

Cell viability and the eventual cytotoxicity of the CHT, PLLA and PLLA+CHT microspheres (in a 1:1 volume ratio) were studied *in vitro* using murine RAW264.7 macrophage. This cell line constitute an excellent model for studies of cytotoxicity of different substances on biological systems, because RAW264.7 expresses different markers of cellular activity, such as, interleukin synthesis, nitric oxide production (NO), expression of nitric oxide synthases (NOS) against toxic substances [21]. These cells were maintained in DMEM without phenol

red supplemented with 10% FBS and antibiotics (100 U/mL penicillin and 100 g/mL streptomycin) at 37°C in a 5% CO_2 atmosphere. The polymeric microspheres were sterilized with ethanol (70% v/v) overnight. Then, they were washed three times with mili-Q water sterile and were incubated with DMEM without phenol red, 10% FBS and antibiotics overnight at 4°C before its use. Cell viability was evaluated by the 3-(4,5-dimethylthiazol-2-yl)-2,5-diphenyl tetrazolium bromide (MTT) assay [17]. Briefly, 1×10^5 cells/tube were seeded inside 500 µl eppendorf tubes with the microspheres and cultured during 24 or 48 h. After these culture periods, cells were incubated for two additional hours with a solution of 0.1 mg/mL MTT (Sigma, USA). After washing, the formazan precipitate was dissolved in 100 µL of dimethyl sulfoxide (DMSO) and the absorbance read at 570 nm using an automatic ELISA plate reader (Infinite® F50, Tecan Trading AG, Switzerland). Results were expressed as % basal, taking as basal the cell viability in the control condition at 24 h. The potential cytotoxicity of the microspheres was evaluated by the interleukin-1β (IL-1β) and the nitric oxide (NO) production released into the culture medium by RAW264.7 cells after 24 and 48 h. IL-1β was measured by ELISA kits (BD OptEIA™ mouse IL-1β ELISA) following the manufacturer's recommendations. The stable end-product of NO production was assessed using Griess reagent [22]. Briefly, 200 µL samples of conditioned media or nitrite standards (0–100 nM) were mixed with 200 µL of Griess reagent (1% sulfanylamide and 0.1% naphthylethylene-diamine in 5% phosphoric acid) and absorbance was measured at 530 nm.

Results are expressed as the mean ± SEM and were obtained from two separate experiments performed in quadruplicate. Differences between groups were assessed by one-way ANOVA with Tukey post hoc test. For non-normal distributed data nonparametrical Kruskal–Wallis with Dunn's post hoc test was performed, using Graph Pad InStat v. 3.00 (Graph Pad Software, San Diego, CA, USA). $p<0.05$ was considered significant for all statistical analyses.

Rabbit model

In order to evaluate cartilage regeneration, an animal model was designed following the ICRS guide [23]. With the approval of the ethics committee of the Universitat de València, 12 week-old male New Zealand rabbits weighing about 1800 g were used. The surgical technique included a medial para-patellar approach to the right knee, eversion of the patella and the creation of the osteochondral injury in the femoral trochlear groove using a 3 mm diameter sized punch. The cartilage defect was filled with wet biomaterial microspheres (with the consistency of a paste), and over them a circular membrane composed of PLLA, 3 mm diameter

and 100 μm thick, was placed. This membrane, with the clot formed by the subchondral bone injury bleeding, ensured mechanical stability without the need for sutures or fibrin glue.

A total of 9 rabbits were used for each experimental group to have results statistically significant. In order to limit the number of experimental animals, only two microspheres formulations were considered: In one of the series, named PLLA, only PLLA microspheres were implanted, in the second series, named PLLA+CHT, a mixture of PLLA and CHT (in a 1:1 volume ratio) was implanted. A different group, named M was used to evaluate the biological ability of the animals to repair the injury, where the cartilage defect was created including the injury of the subchondral bone, but only the PLLA membrane was placed. The control group of native cartilage consisted of the left knees of the rabbits. It must be noted that 2 rabbits deceased during the initial anaesthetic part of the surgery, previous to the implantation of the scaffolds.

12 weeks after the procedure, the animals were sacrificed using a veterinary-controlled tiopental overdose. The knees were extracted and the macroscopic evaluation was carried out following the ICRS proposal [24]. They were then processed, including a fixation in 10% buffered formaldehyde for 5 days followed by decalcification using Osteosoft® for 5 weeks. The samples were then included in polyester-wax for microscopy, low melting-point, and 5 to 7 μm seriated sections were performed. The different sections were stained using Haematoxylin-Eosin (H&E), Toluidine blue and Masson trichromic for the different microscopic measurements. Polarized light microscopy was also used in order to observe the orientation of the collagen fibers.

Microscopic evaluation was also performed following the ICRS II scale [25], where each parameter is scored using a 100 unit visual analogue scale, with a score of 0 being assigned for properties considered indicative of fibrous cartilage or poor quality articular hyaline cartilage, and 100 for good-quality articular hyaline cartilage. However, we added 3 parameters to evaluate the presence of non-reabsorbed membrane and microspheres, as well as inflammation in the areas where they were observed. The quality of the regenerated cartilage obtained was also evaluated using the Image Pro Plus 7.0 programme with morphometric criteria: we measured cartilage and subchondral bone thickness, cell density, interdigitation index (the index obtained by dividing the length of cartilage surface measured in a particular sample and the ideal curved surface a normal cartilage would have), number of non-reabsorbed

microspheres and their depth, area of non-reabsorbed membrane and its depth and, in the cases where they were observed, area and depth of cyst formation or inflammation.

Two independent observers carried out all the measurements, and κ coefficients [26] were calculated in order to establish the consistency of the observations.

The statistical analysis included a Kolmogorov-Smirnov test to determine the normal distribution of the data, R-Pearson test to establish the absence of correlation between variables, Anova test for mean comparison, Chi2 test for categorical variables and Scheffe or Games-Howell test for multiple mean comparisons depending on whether the variances were homogeneous or not. Significant differences were established below $p<0.05$.

Results

Supporting biomaterials

Figure 1 shows the morphology of the PLLA and CHT microspheres. The diameter was 40 ±20 μm for PLLA and 205±5 μm for CHT. The combination of the rigid and hydrophobic microspheres of PLLA with the hydrophilic ones of CHT allows modulating the biomechanical environment found by the cells that invade the site of the cartilage defect. The mechanical confined compression test aims to simulate the situation that occurs *in vivo*, with the implanted microspheres in the cartilage defect. In this test the microspheres are introduced into the poly(tetrafluor ethylene), PTFE cylinder (inset in Figure 2), to a thickness of 1 mm, and distilled water is added to fill the space between the microspheres. The stress-strain diagram (Figure 2) of the test carried out with CHT microspheres shows how, at the beginning, with a tension close to 0, the piston moves, eliminating the excess water (I). In a second stage (II), the applied force grows when the microspheres contact each other and start to deform, and is the stage II that has been considered representative of the elastic modulus during the regeneration process. The origin of deformation was detected by the shift of the stress-strain curve from the straight line fitted to the experimental data in stage I. When the microspheres occupy all the volume, the tension grows rapidly representing the elastic modulus of the block material (III). The value of the compression module was calculated in the strain interval between 0.1 and 0.2 that corresponds to the physiological deformation of cartilage. The values obtained were 1.2±0.25 *MPa* in the case of PLLA, 0.64±0.03 *MPa* for the mixture of PLLA and CHT microspheres and 0.21±0.08 *MPa* for CHT.

In vitro tests, induction of inflammation mediators

As a first step, before implantation of the biomaterial in the animals, inflammatory response was tested *in vitro*. We evaluated cell viability of RAW264.7 macrophages with the different microspheres compared to spheres-free culture (control condition). Figure 3 shows no significant differences in viability of cells cultured in the presence of different microspheres and the control condition, after 24 or 48 h of incubation. The influence of microspheres on the inflammatory response was evaluated by measuring the pro-inflammatory cytokines IL-1β and the NO production by macrophages in culture. We found no differences on IL-1β produced after the cells were grown in the presence or absence (control condition) of microspheres after 24 or 48 h (Figure 4a). Similar results were obtained for NO produced (Figure 4b), although we only found a significant increase in NO production after 48 h of incubation of cells grown in the presence of PLLA+CHT respect to the control (Figure 4b, $p<0.05$).

Rabbit knee model

No inflammatory reaction or infection was observed throughout the post-operative period, and all of the animals were found to have a normal walking behaviour and were able to maintain bipedalism within three weeks after the procedure.

Figure 5 shows representative histology images of the regenerating zone three months after implantation of only PLLA microspheres (Figure 5a) or a mixture of PLLA and CHT microspheres (5c), in both cases covered by a PLLA membrane. The histology of the new-formed tissue when only the membrane was implanted after osteochondral injury is shown in Figure 5d. It is worth noting that the degradation time of PLLA is much longer than three months, thus, both the PLLA membrane and PLLA microspheres are expected to be in the regeneration zone yet. Interestingly enough both are shifted out of the cartilage zone, as observed in Figure 5a (microspheres are indicated by the yellow arrows) and at higher magnification in Figure 5b, while the rests of the membrane are shown by the green arrows. The number of particles shown in the histology when a 50/50 mixture of PLLA and CHT microspheres is implanted is much smaller than when only PLLA microspheres are implanted, and they appear at a larger distance to the articular surface. A macroscopic view of the articular surface three months after implantation is shown in Figure 6. The areas of regenerated cartilage in PLLA series had a smooth white-coloured surface, with only occasional irregularities or small lumps (Figure 6a). Cross section also shows a quite homogeneous cartilage layer in the regeneration site (Figure 6b). Nevertheless, when PLLA and CHT microspheres were implanted irregularities, in the form of lumps, at the surface were more frequent, appearing even at some

distance from the site of the cartilage defect (Figure 6c). The histology of these lumps is shown in Figure 7b and corresponds to a disordered growth of cartilaginous tissue. Group M had a very irregular surface in 75% of the cases, having generally a fibrous appearance, showing a repaired surface with a matt appearance, bulges and filiform projections and occasionally fissures between native and repaired tissues.

Subchondral cysts present in the PLLA and CHT group were present in 44.4% of the PLLA+CHT samples, at a main depth of 2421±979 μm from the surface, and had a mean area of $3{,}6\pm0.96\times10^{6}$ μm^2.

Discussion

There are currently many researches on microspheres use in regenerative medicine and delivery drugs. However, little is known about the influence of the nature of polymers commonly used to prepare microspheres on their interaction with macrophages, and on the release induction of inflammation mediators [20]. Macrophages are a very sensitive culture model to evaluate possible *in vitro* inflammatory responses to a material with potential application in regenerative medicine [16,17,21,22].

Several researchers have also reported good results on the cell viability of osteoblasts [27], chondrocytes [18] and stromal cells [15] cultured in the presence of microspheres, similarly to the present study. In addition, Zan *et al*. did not find significant differences in cell viability when the cells grow with CHT microspheres even after 10 days of culture [27].

Luzardo-Alvarez *et al*. also studied of NO production for RAW264.7 macrophages with CHT microspheres [28]. They found that CHT did not induce significant levels of NO production as compared with control condition, but when cells were stimulated with lipopolysaccharide (LPS) produced levels of NO were six times higher than those of the control. They also evaluated the effect of CHT microspheres to macrophages on tumor necrosis factor alpha (TNF-α) production and found that this cytokine was unaffected by the treatment.

Altogether, our results suggest that the microspheres do not induce cytotoxicity effects on macrophages during the times tested. Macrophages are the first line of defence and recognition of foreign substances and microorganisms [29], hence the importance of our results. This hypothesis, however, was later confirmed using the *in vivo* model.

Rabbit knee model has been widely used as *in vivo* model for articular cartilage regeneration [30,31]. Our group has previously studied the regeneration of articular cartilage in a rabbit knee

model using the combination of a macroporous implant and the stimulation of the subchondral bone by microfracture [10,12,13,14]. The results pointed to the displacement of the implanted biomaterial out of the area of regeneration penetrating the subchondral bone, allowing a tissue with the histological characteristics of the hyaline cartilage to form between the scaffold and the articular surface. This is a very promising result because, on the one hand, it allows the organization of the new formed tissue without the impediment of the presence of the scaffolding material and, on the other hand, the degradation time of the biomaterial needs not to be adjusted (can be longer) to the regenerated cartilage formation. In this study we intend to continue in this line, making it easier for the new tissue to move the supporting biomaterial and acquire the proper organization of the hyaline cartilage.

Particles displacement is more effective in this case. For sure, PLLA microspheres are not reabsorbed, but there are no proofs about degradation of CHT microspheres that could be inserted into the cysts (as we will see below) formed in the subchondral cancellous bone area. The shift of the biomaterial out of the cartilage regeneration zone allows the organization of the new-formed cartilage with the characteristic ordering of hyaline cartilage, with chondrocytes isolated in lacunae and aligned in columns perpendicular to the articular surface. In this way, articular surface has a smooth appearance in the macroscopic view (Figure 6). Microspheres displacement was found in all the cases with a single exception in one case when only PLLA microspheres were implanted, and PLLA remaining microspheres appeared into the new formed cartilage.

Dynamic compression in the site of the regeneration should play an important role in the remodelling of the regeneration site along time. In a previous work [12], we followed the invasion of the cartilage defect along time in a rabbit knee model in which a scaffold was implanted in the cartilage defect after injuring subchondral bone. Just one week after implantation a layer of cells and extracellular matrix was formed at the articular surface attached to the scaffold external surface, and this layer became thicker as regeneration time increased. At the same time, the scaffold pores were invaded by cells. In the present study, we have data only for the regeneration time of three months, but the fact that the membrane that covers the defect is pushed down towards subchondral bone suggests the initial formation of a layer of tissue on top of the practiced cartilage defect.

A comparison of the quality of the regenerated cartilage after implantation of PLLA, PLLA+CHT or no microspheres is performed on the basis of macroscopic and microscopic

evaluation. Since two exitus occurred, the lack of new animals that would qualify for the methodology used within the established time frames justifies the difference in group sizes (7 in group PLLA *vs* 9 in group PLLA+CHT).

Macroscopic evaluation

Individual scores for each category and group are summed up in Table 1. PLLA series obtained the highest mean score (10.59±0.79), PLLA+CHT obtained a slightly lower mean score (9.38±1.51), group M had the lowest mean score (8.50±1.29), and control group obtained maximum scores (12) as it was expected. Significant differences were observed in PLLA series ($p=0.018$) for the macroscopic appearance category, resulting in better scores.

All intraobserver Kappa correlation index (κ) for macroscopic evaluation were found to be 'moderate' or higher, with 62.5% of the results having a correlation of 'substantial' or 'almost perfect'. Interobserver κ were found to be 'fair' or 'moderate'.

Significant differences were observed in the category macroscopic surface assessment, with higher results in PLLA series (Table 1). This implies a more regular surface, with absence of fissures or fibrillations. All of the experimental groups' totals were in the range 8-11, thus being described as "nearly normal" regeneration cartilage by the ICRS scale. However, PLLA series was in the upper limit, whilst both groups PLLA+CHT and M obtained totals that placed them in the lower limit of the grade. This is due to sufficient thickness and integration of the repaired or regenerated tissue in all groups, and does not imply a hyaline-like cartilage.

Microscopic evaluation

Histological parameters are listed in Table 2. In all of the experimental groups, a small invagination was observed where the reparative/regenerative area and the native cartilage met. An increase in the vascularization of the subchondral bone was also noted in comparison to that of native cartilage. Whenever there were different qualities of cartilage regeneration obtained, seriated samples were taken and the scores were calculated with those considered more representative.

PLLA series had a slightly thicker cartilage, with better tissue architecture in the areas nearest to the native cartilage. Its cell morphology was normal, with chondrocytes having a basophilic cytoplasm and no apparent morphological changes. Chondrocyte clustering was generally observed both in the peripheral areas of regenerated cartilage and the adjacent native areas (Figure 5a).

In the PLLA+CHT group, normal cellularity was also observed, with a slightly thicker regeneration cartilage and the presence of clustering, besides the appearance of lumps aformentioned. It is worth note the formation of subchondral cysts in 66.7% of the cases (Figure 7a), with multinucleated cells and remains of membranes and biomaterials within them. These cysts appear quite far from the articular surface deep in the subchondral spongy bone tissue, which might weaken the joint. The series M obtained poor cartilage regeneration, similar to a fibrous repair. Cartilage thickness was variable, with cases of increases or decreases with respect to native one. The tissue obtained was poorly organised and the surface was found to be generally irregular (Figure 5d).

All interobserver κ for macroscopic evaluation were found to be 'fair' or higher, with 68.5% of the results having a correlation of 'substantial' or 'almost perfect'.

Significant differences were observed in the categories tissue morphology, surface architecture and superficial assessment. In them, group M had significantly lower scores compared to groups PLLA or PLLA+CHT. No significant differences were found between PLLA and PLLA+CHT series and native cartilage (control group), suggesting a high quality regeneration cartilage.

The categories added to the ICRS II score to evaluate material reabsorption had a significant difference in PLLA microsphere presence. However, the presence of subchondral cysts was only observed in PLLA+CHT. A possible explanation would be that biomaterials were reabsorbed at a similar rate, but whereas PLLA was found as microspheres, CHT would have been dragged into these cysts in the subchondral bone, probably originating from an immune response already described in literature with biomaterials [8,9], although our *in vitro* experiments only showed an increase in NO production in PLLA+CHT group after 24 h of culture.

It must be noted that the time of evolution of the regeneration prior to the sacrifice of the rabbits was 12 weeks. This time was decided as it is within the range established by the ICRS [32], and longer times do not seem to improve the quality of cartilage regeneration [33,34]. Nevertheless, it is shorter than the half-life of both PLLA and CHT, so presence of the biomaterial in the samples was expected. Further studies with different evolution times could clarify the matter.

Differences were also found in surface architecture and surface assessment, having significantly worse results in group M. This was further demonstrated by significantly better values of interdigitation index in groups PLLA, PLLA+CHT and Control to group M, whilst no differences were observed when comparing groups PLLA and PLLA+CHT to the control

group. Hence, microspheres scaffolding with PLLA and CHT results in a tissue whose surface is both microscopically and numerically equivalent to normal hyaline cartilage.

Morphometric evaluation

Individual morphometric values for each category and group are summarized up in Table 3. Some parameters lack clear reference values in literature, and hence must be approached with care. Cell density increases both in immature cartilage and in fibrocartilage, an increase observed in M series with respect to the native cartilage was expected, but the increase observed in group PLLA+CHT and M and the decrease observed in group PLLA have unclear meaning. Chondrocyte clustering was also described as a negative feature associated with degeneration in ostheoarthritic tissue [11]. Other studies interpret these clusters as a sign of immature cartilage during the healing process [33,35,36]. Regenerated tissues were generally thicker than native cartilage, as was the subchondral bone beneath them. Interdigitation index showed significantly lower values in control group, with no differences observed in groups PLLA, PLLA+CHT and M.

Conclusions

The regeneration of the articular cartilage requires both the presence of cells with chondrogenic capacity in the site of the defect and a mechanical support capable to transmit to the cells the dynamic compression efforts to which the cartilage is subjected *in vivo*, so as to stimulate the characteristic organization of the hyaline cartilage. In the regeneration strategy presented in this paper, mesenchymal stem cells come from the microfracture of subchondral bone, while the role of the mechanical support is made by the microspheres, either PLLA or a mixture of PLLA and CHT. In both cases, the histological characteristics of the regenerated tissue are those of the hyaline cartilage that can grow with its characteristic arrangement thanks to the simultaneous displacement of the implanted microspheres towards the subchondral bone. Interestingly enough, even the membrane that was placed covering the microspheres at the time of the intervention is also displaced towards subchondral bone. The system is very promising as a strategy of regeneration, however, the presence of chitosan has produced certain anomalous effects, such as the formation of lumps on the articular surface outside the region where the defect was created and which have the structure of a cartilaginous disordered tissue, and also the formation of cysts in the bone at a considerable distance from the articular surface. It is noteworthy that neither the CHT nor the PLLA micro-spheres gave any inflammatory response that could be highlighted in the trials carried out on cultures with macrophages.

Acknowledgements: Financial support from the Spanish Ministry of Economy and Competitiveness (MINECO) through the project MAT2016-76039-C4-(1 and 2)-R (Agencia Estatal de Investigación/Fondo Europeo de Desarrollo Regional de la Unión Europea) is acknowledged (Spanish group). This work was also partially supported by grats from Comisión de Investigaciones Científicas de la Provincia de Buenos Aires (CICPBA), Universidad Nacional de La Plata, Proyecto 11/X643 (Argentina group). The consorcio Centro de Investigación Biomédica en Red, Bioingeniería, Biomateriales y Nanomedicina, CIBER-BBN is an initiative funded by the VI National R&D&I Plan 2008–2011, Iniciativa Ingenio 2010, Consolider Program. CIBER Actions are financed by the Instituto de Salud Carlos III with assistance from the European Regional Development Fund. M.L.L. is a Doctoral Fellow of Universidad Nacional de La Plata, J.M.F. is Investigador Adjunto of the Consejo Nacional de Investigaciones Científicas y Técnicas, CONICET, and A.M.C. is Investigador Principal de la Comisión de Investigaciones Científicas de la Provincia de Buenos Aires, CICPBA.

References

1. Carmona L, Ballina J, Gabriel R. The burden of musculoskeletal diseases in the general population of Spain: results from a national survey. Ann Rheum Dis 2001; 60:1040–1045

2. Allepuz A, Martínez O, Tebé C, Nardi J, Portabella F, Espallargues M. Joint registries as continuous surveillance systems: The experience of the catalan arthroplasty register (RACat). J Arthroplasty 2014; 29:484–490

3. Steadman JR, Rodkey WG, Briggs KK, Rodrigo JJ. The microfracture technic in the management of complete cartilage defects in the knee joint. Orthopade 1999; 28:26-32

4. Hangody L, Kish G, Kárpáti Z, Udvarhelyi I, Szigeti I, Bély M. Mosaicplasty for the treatment of articular cartilage defects: application in clinical practice. Orthopedics 1998; 21:751-756

5. McCormick F, Harris JD, Abrams GD, Frank R, Gupta A, Hussey K, Wilson H, Bach B Jr, Cole B. Trends in the surgical treatment of articular cartilage lesions in the United States: An analysis of a large private-payer database over a period of 8 years. Arthroscopy 2014; 30:222-226

6. Goyal D, Keyhani S, Lee EH, Hui JH. Evidence-based status of microfracture technique: a systematic review of level I and II studies. Arthroscopy 2013; 29:1579–88

7. Zhang C, Cai YZ, Lin XJ. One-step cartilage repair technique as a next generation of cell therapy for cartilage defects: biological characteristics, preclinical application, surgical techniques, and clinical developments. Arthroscopy 2016; 32:1444-1450

8. Chu J, Zeng S, Gao L, Groth T, Li Z, Kong J, Zhao M, Li L. Poly (L-lactic acid) porous scaffold-supported alginate hydrogel with improved mechanical properties and biocompatibility. Int J Artif Organs 2016; 39(8):435–43

9. Conoscenti G, Schneider T, Stoelzel K, Carfì Pavia F, Brucato V, Goegele C, La Carrubba V, Schulze-Tanzil G. PLLA scaffolds produced by thermally induced phase separation (TIPS) allow human chondrocyte growth and extracellular matrix formation dependent on pore size. Mater Sci Eng C 2017; 80:449–59

10. Martinez-Diaz S, Garcia-Giralt N, Lebourg M, Gómez-Tejedor JA, Vila G, Caceres E, Benito P, Pradas MM, Nogues X, Ribelles JL, Monllau JC. In vivo evaluation of 3-dimensional polycaprolactone scaffolds for cartilage repair in rabbits. Am J Sports Med 2010; 38(3):509-519

11. Vikingsson L, Sancho-Tello M, Ruiz-Saurí A, Martínez Díaz S, Gómez-Tejedor JA, Gallego Ferrer G, Carda C, Monllau JC, Gómez Ribelles JL. Implantation of a polycaprolactone scaffold with subchondral bone anchoring ameliorates nodules formation and other tissue alterations. Int J Artif Organs 2015; 38(12):659-666

12. Sancho-Tello M, Forriol F, Gastaldi P, Ruiz-Saurí A, Martín De Llano JJ, Novella-Maestre E, Antolinos Turpín, CM, Gómez Tejedor JA, Gómez Ribelles JL, Carda C. Time evolution of in vivo articular cartilage repair induced by bone marrow stimulation and scaffold implantation in rabbits. Int J Artif Organs 2015; 38(4):210–23

13. Sancho-Tello M, Forriol F, Martín de Llano JJ, Antolinos-Turpin C, Gómez-Tejedor JA, Gómez Ribelles JL, Carda C. Biostable scaffolds of polyacrylate polymers implanted in the articular cartilage induce hyaline-like cartilage regeneration in rabbits. Int J Artif Organs 2017; 40(7):350-357

14. Lebourg M, Martínez-Díaz S, García-Giralt N, Torres-Claramunt R, Gómez-Tejedor JA, Ribelles JL, Vila-Canet G, Monllau JC. Cell-free cartilage engineering approach using hyaluronic acid-polycaprolactone scaffolds: a study in vivo. J Biomater Appl 2014; 28(9):1304-1315

15. García Cruz DM, Escobar Ivirico JL, Gomes MM, Gómez Ribelles JL, Salmerón Sánchez M, Reis RL, Mano JF. Chitosan microparticles as injectable scaffolds for tissue engineering. Tissue Eng Regen Med 2008; 2(6):378-380

16. Lastra ML, Molinuevo MS, Blaszczyk-Lezak I, Mijangos C, Cortizo MS. Nanostructured fumarate copolymer-chitosan crosslinked scaffold: An in vitro osteochondrogenesis regeneration study, J Biomed Mater Res A 2018; 106(2):570-579

17. Lastra ML, Molinuevo MS, Cortizo AM, Cortizo MS. Fumarate copolymer-chitosan cross-linked scaffold directed to osteochondrogenic tissue engineering. Macromol Biosci 2017; 17(5):1600219

18. Lao L, Tan H, Wang Y, Gao C. Chitosan modified poly (L-lactide) microspheres as cell microcarriers for cartilage tissue engineering. Colloids Surf B Biointerfaces 2008; 66(2):218-225

19. Almeida CR, Serra T, Oliveira MI, Planell JA, Barbosa MA, Navarro M. Impact of 3-D printed PLA- and chitosan-based scaffolds on human monocyte/macrophage responses: unraveling the effect of 3-D structures on inflammation. Acta Biomater 2014; 10(2):613-622

20. Bitencourt Cda S, Silva LB, Pereira PA, Gelfuso GM, Faccioli LH. Microspheres prepared with different co-polymers of poly(lactic-glycolic acid) (PLGA) or with chitosan cause distinct effects on macrophages. Colloids Surf B Biointerfaces 2015; 136:678-686

21. Denlinger LC, Fisette PL, Garis KA, Kwon G, Vazquez-Torres A, Simon AD, Nguyen B, Proctor RA, Bertics PJ, Corbett JA. Regulation of inducible nitric oxide synthase expression by macrophage purinoreceptors and calcium. J Biol Chem 1996; 271:337–342

22. Fernández JM, Cortizo MS, Cortizo AM. Fumarate/ceramic composite based scaffolds for tissue engineering: evaluation of hydrophylicity, degradability, toxicity and biocompatibility. J Biomater Tissue Eng 2014; 4(3):227-234

23. Hoemann C, Kandel R, Roberts S, Saris DBF, Creemers L, Mainil-Varlet P, Méthot S, Hollander AP, Buschmann MD. International Cartilage Repair Society (ICRS) recommended guidelines for histological endpoints for cartilage repair studies in animal models and clinical trials. Cartilage 2011; 2(2):153–72

24. Van den Borne MPJ, Raijmakers NJH, Vanlauwe J, Victor J, de Jong SN, Bellemans J, Saris DB. International Cartilage Repair Society (ICRS) and Oswestry macroscopic cartilage

evaluation scores validated for use in Autologous Chondrocyte Implantation (ACI) and microfracture. Osteoarthr Cartil 2007; 15(12):1397–402

25. Mainil-Varlet P, Van Damme B, Nesic D, Knutsen G, Kandel R, Roberts S. A new histology scoring system for the assessment of the quality of human cartilage repair: ICRS II. Am J Sports Med 2010; 38(5):880–90

26. Landis JR, Koch GG. The measurement of observer agreement for categorical data. Biometrics 1977; 33(1):159

27. Zan Q, Wang C, Dong L, Cheng P, Tian J. Effect of surface roughness of chitosan-based microspheres on cell adhesion. Applied Surface Science 2008; 255(2):401-403

28. Luzardo-Alvarez A, Blarer N, Peter K, Romero JF, Reymond C, Corradin G, Gander B. Biodegradable microspheres alone do not stimulate murine macrophages in vitro, but prolong antigen presentation by macrophages in vitro and stimulate a solid immune response in mice. J Control Release 2005; 109(1-3):62-76

29. Gordon S. The macrophage: past, present and future. Eur J Immunol 2007; 37:S9

30. Bonasia DE, Martin JA, Marmotti A, Kurriger GL, Lehman AD, Rossi R, Amendola A. The use of autologous adult, allogenic juvenile, and combined juvenile-adult cartilage fragments for the repair of chondral defects. Knee Surg Sports Traumatol Arthrosc 2016; 24(12):3988-3996

31. Dashtdar H, Murali MR, Abbas AA, Suhaeb AM, Selvaratnam L, Tay LX, Kamarul T. PVA-chitosan composite hydrogel versus alginate beads as a potential mesenchymal stem cell carrier for the treatment of focal cartilage defects. Knee Surg Sports Traumatol Arthrosc 2015; 23(5):1368-1377

32. Zhu W, Chen K, Lu W, Sun Q, Peng L, Fen W, Li H, Ou Y, Liu H, Wang D, Zeng Y. In vitro study of nano-HA/PLLA composite scaffold for rabbit BMSC differentiation under TGF-β1 induction. Vitr Cell Dev Biol – Anim 2014; 50(3):214–20

33. Kumar MNVR, Muzzarelli RAA, Muzzarelli C, Sashiwa H, Domb AJ. Chitosan chemistry and pharmaceutical perspectives. Chem Rev 2004; 104(12):6017–84

34. Teté S, Mastrangelo F, Carone L, Nargi E, Costanzo G, Vinci R, Burruano F, Tortorici S, Dadorante V, Caciagli F, Traini T, Gherlone E, Caraffa A, Salini V, Conti P, Ciccarelli R.

Morphostructural analysis of human follicular stem cells on highly porous bone hydroxyapatite scaffold. Int J Immunopathol Pharmacol 2007; 20(4):819–26

35. Bell AD, Hurtig MB, Quenneville E, Rivard G-É, Hoemann CD. Effect of a rapidly degrading presolidified 10 kDa chitosan/blood implant and subchondral marrow stimulation surgical approach on cartilage resurfacing in a sheep model. Cartilage 2017; 8(4):417–31

36. Kuo TF, Lin MF, Lin YH, Lin YC, Su RJ, Lin HW, Chan WP. Implantation of platelet-rich fibrin and cartilage granules facilitates cartilage repair in the injured rabbit knee: preliminary report. Clinics 2011; 66(10):1835–8

Captions to Figures

Fig. 1 (a) FESEM picture of poly(L-lactic acid), PLLA, microspheres produced by an oil/water emulsion (dimension bar 20 μm, the diameter of these microspheres was 40 ± 20 μm, mean ± standard deviation); (b) binocular loupe pictures of chitosan, CHT, microspheres produced by neutralization of the CHT acidic solution swollen in water (dimension bar 200 μm, the diameter of these microspheres was 205 ± 5 μm, mean ± standard deviation)

Fig. 2 Stress-strain compression test of the wet microspheres confined in a plunger cylinder device (see text). (•) Chitosan, CHT, (▬) poly(L-lactic acid), PLLA (■) PLLA+CHT

Fig. 3 MTT assay results expressed as % basal, taking as basal the cell viability in the control condition at 24 h. RAW 264.7 macrophages cultured for 24 and 48 h with chitosan, CHT, poly(L-lactic acid), PLLA and CHT+PLLA microspheres. Data represent the mean ± SEM

Fig. 4 Cytotoxicity assay. Production of interleukin-1β, IL-1β (a) and NO (b) by RAW 264.7 macrophages upon incubation with different microspheres. Data represent the mean ± SEM. *$p<0.05$ vs control

Fig. 5 Microscopic views of the experimental areas for groups (a) poly(L-lactic acid), PLLA (H&E), (b) PLLA sample with higher magnification showing the remaining microspheres and membrane located in subchondral bone (H&E), (c) PLLA+chitosan, PLLA+CHT (H&E), (d) series M (H&E), (e) sample of group PLLA+CHT stained with toluidine blue in order to evaluate metachromasia, (f) image viewed under polarized light microscopy of a sample of the PLLA group. White arrows show the limit of the practiced cartilage defect, yellow arrows and green arrows indicate some of the PLLA microspheres and the membrane remaining after three-months implantation. Individual scores in the ICRS II scale for each category and group are summed up in Table 2

Fig. 6 Macroscopic visualization of the regenerated cartilage, (a) and (b) frontal and cross section views after implantation of poly(L-lactic acid), PLLA microspheres covered by the membrane, (c) implantation of PLLA and chitosan, CHT microspheres, (d) only microfracture of subchondral bone covered by the membrane. Arrowheads point some of the superficial lumps

Fig. 7 Histological views (H&E) showing (a) the formation of cysts and (b) lumps in the articular surface in poly(L-lactic acid) + chitosan, PLLA+CHT series

Tables

Table 1. ICRS macroscopic evaluation of cartilage repair. Data are presented as mean ± SD. Statistical significance was determined by Chi2 test, and $p<0.05$ was considered statistically significant. Results for native cartilage are not presented, as they were always maximum (4 in each category, with a total of 12), as to be expected from hyaline cartilage.

Table 2. ICRS II scale. Each parameter is scored using a 100 unit visual analogue scale, with a score of 0 being assigned for properties considered indicative of fibrous cartilage or poor quality articular hyaline cartilage, and 100 for good-quality articular hyaline cartilage, and are presented as mean ± SD. Statistical significance was determined by Chi2 test, and $p<0.05$ was considered statistically significant. Results for control group are not presented, as they were always maximum (100), as to be expected from hyaline cartilage. Tidemark values are not included as they could not be measured. Mean ICRS II were calculated with the other 13 parameters.

Table 3. Morphometrical parameters measured. * $P<0.05$

Category	PLLA	PLLA+CHT	Membrane (M)
Degree of defect repair	3.86±0.38	3.25±0.89	3.25±0.96
Integration to border zone	3.00±0.00	3.38±0.52	2.75±0.50
Macroscopic appearance	3.71±0.76*	2.75±0.46	2.50±1.29
Total	10.57±0.79	9.38±1.51	8.50±1.29
Grade	II	II	II

Table 1. ICRS macroscopic evaluation of cartilage repair. Data are presented as mean ± SD. Statistical significance was determined by Chi2 test, and $p<0.05$ was considered statistically significant. Results for native cartilage are not presented as they were always maximum (4 in each category, with a total of 12), as to be expected from hyaline cartilage.

Histological parameter	PLLA	PLLA+CHT	Membrane
Tissue morphology	75.0±14.4	86.1±18.2	25.0±28.9*
Matrix staining	53.6±33.6*	88.9±13.2	18.8±12.5*
Cell morphology	78.6±30.4	94.4±9.4	31.3±31.5
Chondrocyte clustering	75.0±14.4	75.0±37.5	50.0±45.6
Surface architecture	96.4±9.4	86.1±18.2	25.0±35.4*
Basal integration	67.9±37.4	77.8±26.4	62.5±43.3
Marrow fibrosis	100.0±0.0	86.1±33.3	93.8±12.5
Inflammation	100.0±0.0	97.2±8.3	75.0±50.0
Abnormal calcification	100.0±0.0	100.0±0.0	100.0±0.0
Vascularization	96.4±9.4	100.0±0.0	100.0±0.0
Surface assessment	82.1±18.9	83.3±12.5	12.5±14.4*
Mid/deep zone assessment	78.6±17.3	72.2±31.7	31.3±37.5
Overall assessment	78.6±17.3	80.6±20.8	31.3±37.5
Mean ICRS II	83.2±9.7	86.8±10.6	50.5±20.6

Table 2. ICRS II scale. Each parameter is scored using a 100 unit visual analogue scale, with a score of 0 being assigned for properties considered indicative of fibrous cartilage or poor quality articular hyaline cartilage, and 100 for good-quality articular hyaline cartilage, and are presented as mean ± SD. Statistical significance was determined by Chi2 test, and $p<0.05$ was considered statistically significant. Results for control group are not presented, as they were always maximum (100), as to be expected from hyaline cartilage. Tidemark values are not included as they could not be measured. Mean ICRS II were calculated with the other 13 parameters.

Morphometry parameter	PLLA	PLLA+CHT	Membrane	Native
Cartilage thickness (μm)	705±292	711±215	670±244	478±94
Subchondral bone thickness (μm)	786±195	720±225	566±193	650±235
Cell density (cells/mm^2)	1498±149	2366±1041	2579±1490	1914±466
Interdigitation index	1.14±0.10	1.28±0.14	1.73±0.60*	1.03±0.02

Table 3. Morphometrical parameters measured. * P<0.05

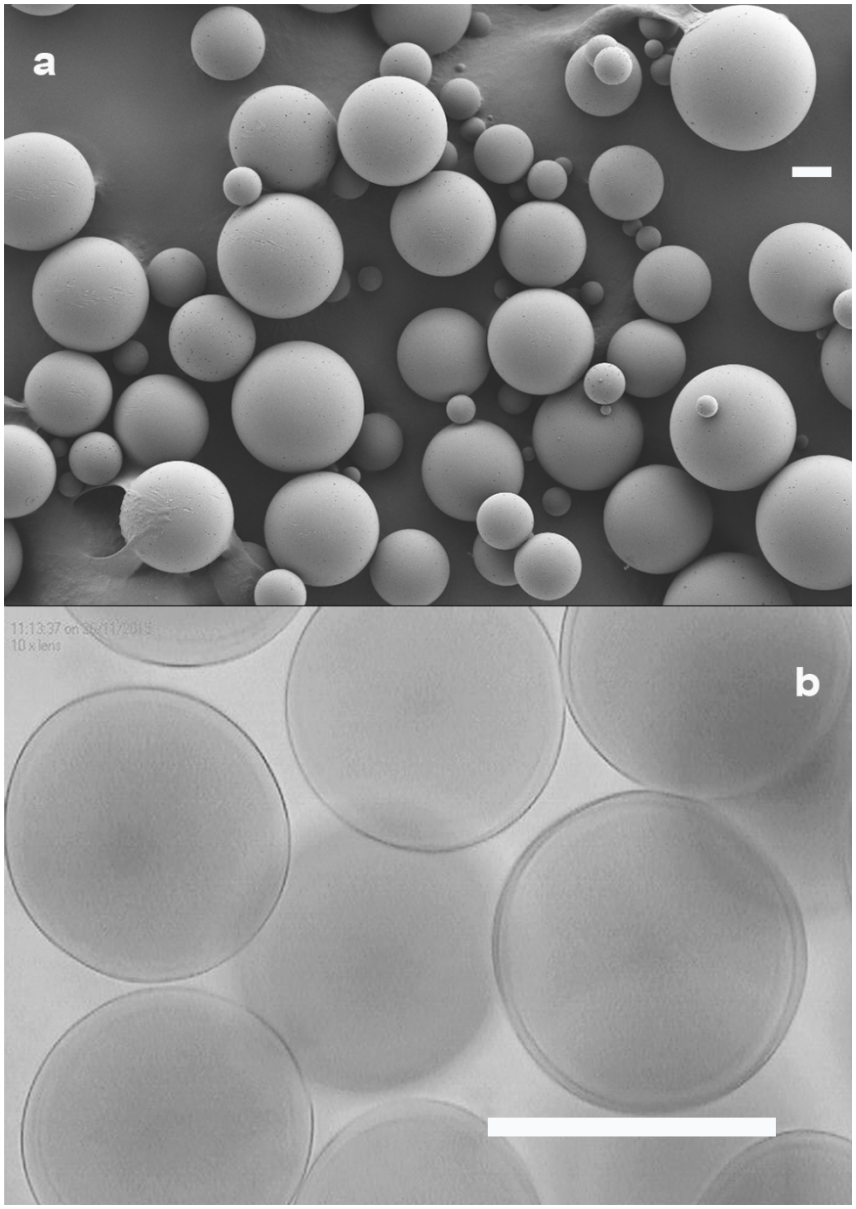

Fig. 1 (a) FESEM picture of poly(L-lactic acid), PLLA, microspheres produced by an oil/water emulsion (dimension bar 20 μm, the diameter of these microspheres was 40 ± 20 μm, mean ± standard deviation); (b) binocular loupe pictures of chitosan, CHT, microspheres produced by neutralization of the CHT acidic solution swollen in water (dimension bar 200 μm, the diameter of these microspheres was 205 ± 5 μm, mean ± standard deviation)

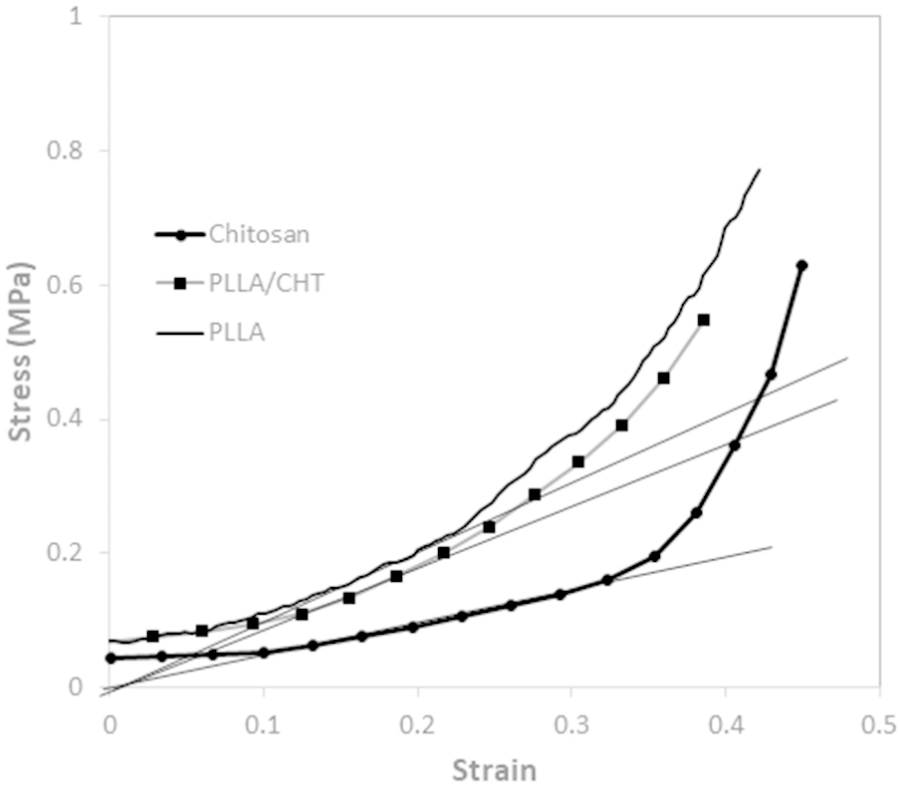

Fig. 2 Stress-strain compression test of the wet microspheres confined in a plunger cylinder device (see text). (•) Chitosan, CHT, (—) poly(L-lactic acid), PLLA (■) PLLA+CHT

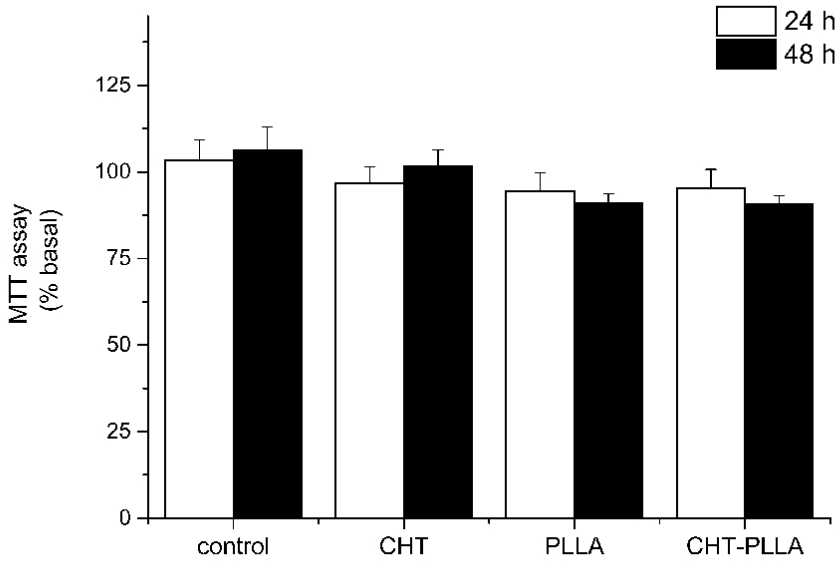

Fig. 3 MTT assay results expressed as % basal, taking as basal the cell viability in the control condition at 24 h. RAW 264.7 macrophages cultured for 24 and 48 h with chitosan, CHT, poly(L-lactic acid), PLLA and CHT+PLLA microspheres. Data represent the mean ± SEM

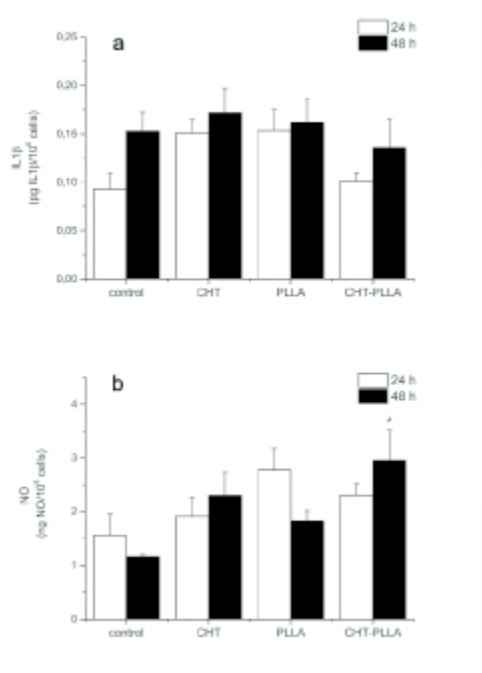

Fig. 4 Cytotoxicity assay. Production of interleukin-1β, IL-1β (a) and NO (b) by RAW 264.7 macrophages upon incubation with different microspheres. Data represent the mean ± SEM. *p<0.05 vs control

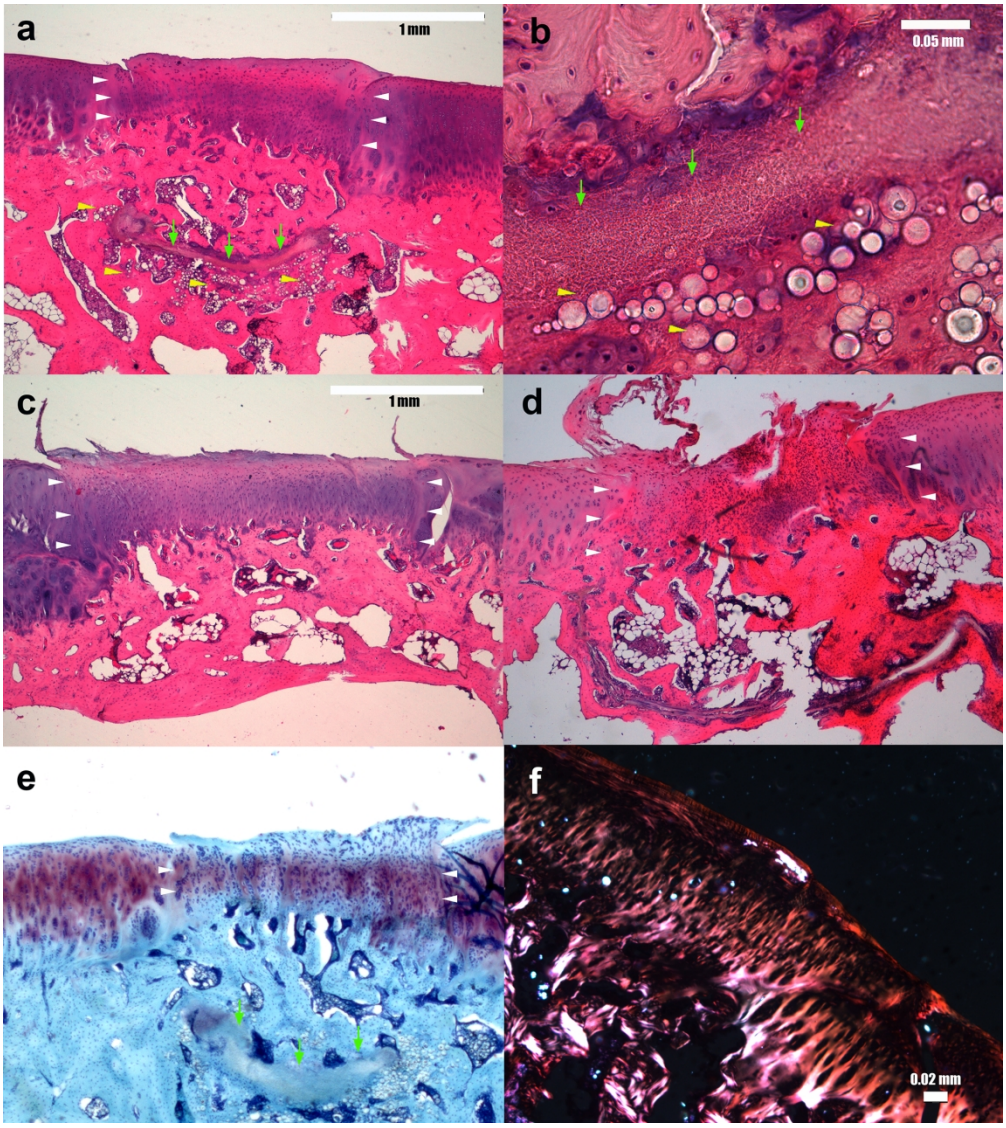

Fig. 5 Microscopic views of the experimental areas for groups (a) poly(L-lactic acid), PLLA (H&E), (b) PLLA sample with higher magnification showing the remaining microspheres and membrane located in subchondral bone (H&E), (c) PLLA+chitosan, PLLA+CHT (H&E), (d) series M (H&E), (e) sample of group PLLA+CHT stained with toluidine blue in order to evaluate metachromasia, (f) image viewed under polarized light microscopy of a sample of the PLLA group. White arrows show the limit of the practiced cartilage defect, yellow arrows and green arrows indicate some of the PLLA microspheres and the membrane remaining after three-months implantation. Individual scores in the ICRS II scale for each category and group are summed up in Table 2

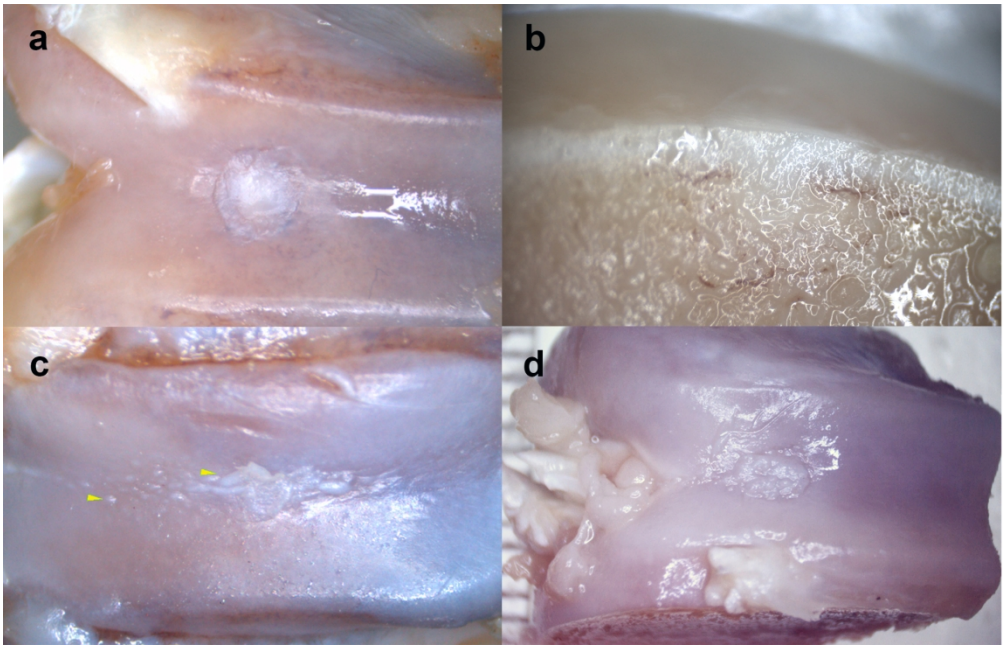

Fig. 6 Macroscopic visualization of the regenerated cartilage, (a) and (b) frontal and cross section views after implantation of poly(L-lactic acid), PLLA microspheres covered by the membrane, (c) implantation of PLLA and chitosan, CHT microspheres, (d) only microfracture of subchondral bone covered by the membrane. Arrowheads point some of the superficial lumps

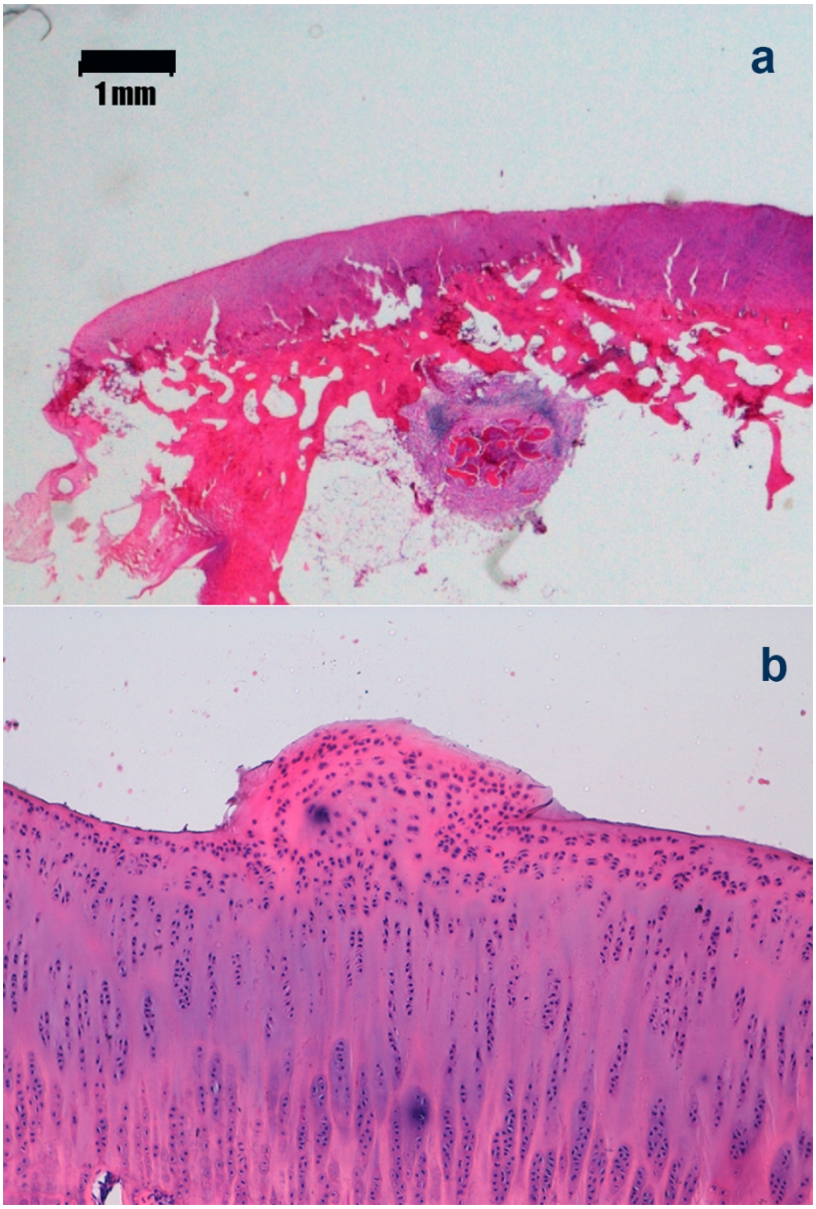

Fig. 7 Histological views (H&E) showing (a) the formation of cysts and (b) lumps in the articular surface in poly(L-lactic acid) + chitosan, PLLA+CHT series